JOURNAL OF AGRICULTURAL AND FOOD CHEMISTRY

J. Agric. Food Chem. **2007,** *55,* 10055–10066 **10055**

Differential Gene Expression in Intestinal Epithelial Cells Induced by Single and Mixtures of Potato Glycoalkaloids

TAFADZWA MANDIMIKA,[†,‡] HAKAN BAYKUS,[†] YVONNE VISSERS,[§] PRESCILLA JEURINK,[∥] JENNEKE POORTMAN,[†] CUTBERTO GARZA,[⊥] HARRY KUIPER,[†] AND AD PEIJNENBURG*[,†]

RIKILT, Institute of Food Safety, Wageningen University and Research Centre, Post Office Box 230, 6700 AE Wageningen, The Netherlands, Division of Nutritional Sciences, Cornell University, Ithaca, New York 14853, WU Agrotechnology and Food Sciences, Wageningen University and Research Centre, Post Office Box 8129, 6700 EV Wageningen, The Netherlands, WU Cell Biology and Immunology, Wageningen University and Research Centre, Post Office Box 9101, 6700 HB Wageningen, The Netherlands, and Office of the Provost, Boston College, Chestnut Hill, Massachusetts 02467

α-Chaconine and α-solanine are naturally occurring toxins. They account for 95% of the total glycoalkaloids in potatoes (*Solanum tuberosum* L.). At high levels, these glycoalkaloids may be toxic to humans, mainly by disrupting cell membranes of the gastrointestinal tract. Gene-profiling experiments were performed, whereby Caco-2 cells were exposed to equivalent concentrations (10 μM) of pure α-chaconine or α-solanine or glycoalkaloid mixtures of varying α-chaconine/α-solanine ratios for 6 h. In addition, lactate dehydrogenase, cell cycle, and apoptosis analyses experiments were also conducted to further elucidate the effects of glycoalkaloids. The main aims of the study were to determine the transcriptional effects of these glycoalkaloid treatments on Caco-2 cells and to investigate DNA microarray utility in conjunction with conventional toxicology in screening for potential toxicities and their severity. Gene expression and pathway analyses identified changes related to cholesterol biosynthesis, growth signaling, lipid and amino acid metabolism, mitogen-activated protein kinase (MAPK) and NF-κB cascades, cell cycle, and cell death/apoptosis. To varying extents, DNA microarrays discriminated the severity of the effect among the different glycoalkaloid treatments.

KEYWORDS: α-Chaconine; α-solanine; cell membrane disruption; DNA microarrays; glycoalkaloids; potatoes

1. INTRODUCTION

α-Chaconine and α-solanine account for 95% of the total glycoalkaloids present in potatoes (*Solanum tuberosum* L.) (*1*). These are naturally occurring toxins, which at high levels (3–6 mg/kg body weight) may have toxic effects on human health (*2*). Both consist of the aglycone solanidine but differ in the carbohydrate side chain attached to the aglycone moiety (**Figure 1**). The branched trisaccharides solatriose (α-L-rhamnopyranosyl-β-D-glucopyranosyl-β-D-galactopyranose) and chacotriose (bis-α-L-rhamnopyranosyl-β-D-glucopyranose) are the carbohydrate side chains of α-solanine and α-chaconine, respectively (**Figure 1**) (*3–5*). α-Chaconine is toxicologically more potent and is usually present at slightly higher concentrations in potatoes than α-solanine. Toxicological differences are attributed to the disparate carbohydrate side chains (*6, 7*).

Toxicological effects of individual glycoalkaloids have been described well in humans. These include gastrointestinal disturbances, increased heart beat, hemolysis, and neurotoxic effects (*8*). Reported toxicities are mainly due to acetylcholinesterase inhibition and cell-membrane disruptive activities that affect digestive and other organs (*9*). Toxicities induced in other species include hepatoxicity in mice (*10*), increased hepatic ornithine decarboxylase activity in rats (*11*), craniofacial malformations in hamsters (*12*), and developmental toxicity in frog embryos (*7, 13*).

* To whom correspondence should be addressed: Toxicology and Effect Monitoring Group, RIKILT, Institute of Food Safety, Wageningen University and Research Centre, Post Office Box 230, 6700 AE Wageningen, The Netherlands. Telephone: + 31-317-475462. Fax: + 31-317-417717. E-mail: ad.peijnenburg@wur.nl.

† RIKILT, Institute of Food Safety, Wageningen University and Research Centre.

‡ Cornell University.

§ WU Agrotechnology and Food Sciences, Wageningen University and Research Centre.

∥ WU Cell Biology and Immunology, Wageningen University and Research Centre.

⊥ Boston College.

10.1021/jf0724320 CCC: $37.00
Published on Web 11/01/2007

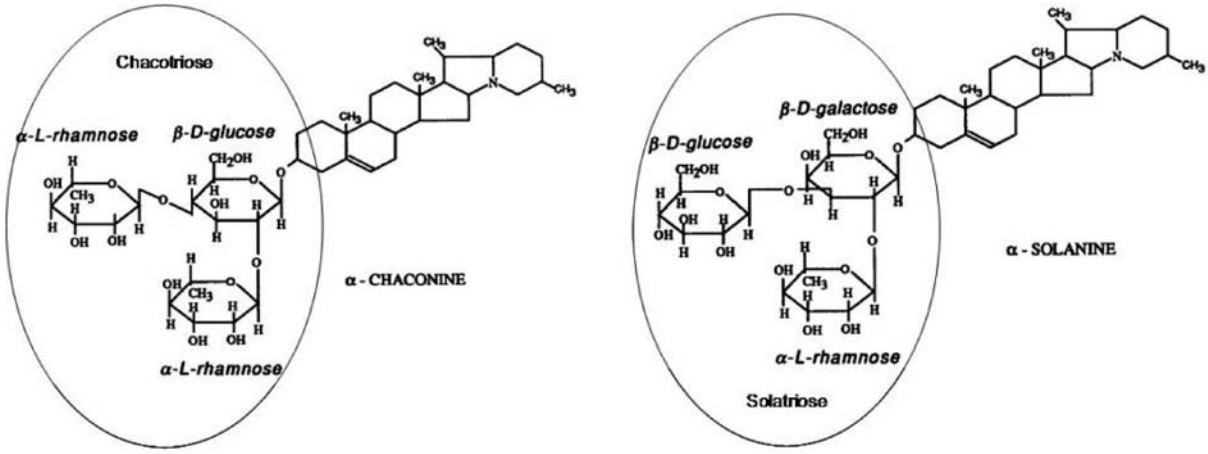

Figure 1. Chemical structures of α-chaconine and α-solanine.

Total glycoalkaloid concentrations of most commercial potatoes are usually below 200 mg/kg of fresh potatoes (*14*) but can increase following light exposure or mechanical injury, for example, from peeling and slicing (*15*). α-Chaconine and α-solanine are present in potatoes at varying concentrations and ratios. In combination, they may interact synergistically, resulting in a level of toxicity that is more severe than is observed when either glycoalkaloid is administered alone (*5*, *13*, *16–18*). Human consumption of potatoes results in the ingestion of α-chaconine and α-solanine in varying ratios, usually ranging from ∼1.2:1 to ∼2.4:1 (α-chaconine/α-solanine), depending upon the specific variety of potato (*17*). Studies have shown that incorporation of an anti-sense transgene encoding either the enzyme solanidine UDP-galactose galactosyltransferase (SGT1) or solanidine UDP-glucose glucosyltransferase (SGT2) in potatoes can result in the downregulation of glycoalkaloid biosynthesis, by reducing the levels of either α-solanine or α-chaconine, respectively (*19*, *20*). Alteration of glycoalkaloid ratios/levels in potatoes may have potentially nutritional/health benefits to consumers. Therefore, from a food safety perspective, assessment of the toxic effects of glycoalkaloid mixtures at varying α-chaconine/α-solanine ratios found in common and possibly transgenic potato varieties would be informative.

Predictions of adverse health effects induced by glycoalkaloid and other toxin mixtures are usually based on data obtained from single compound exposures. Unfortunately, observed toxicities commonly deviate from such predictions. Prediction of adverse effects of whole foods is especially difficult because of the many interactions that may occur among the high number of nutrients and other food substances commonly found in whole foods. Such interactions may alter the degree and possibly the nature of predicted toxic effects of individual food constituents (*21*).

DNA microarrays permit the quantitative simultaneous comparison of the expression of thousands of individual genes in different biological samples. This may facilitate screening, assessment, and/or prediction of putative harmful interactions following exposure to mixtures of substances or whole foods. Thus, changes in gene expression may provide more sensitive, immediate, and comprehensive markers of toxicity than conventional toxicological methods and endpoints (*22*).

The present study focused on the detection and possible significance of multiple gene responses induced by equivalent concentrations of pure α-chaconine or α-solanine or glycoalkaloid mixtures of varying α-chaconine/α-solanine ratios in human intestinal epithelial Caco-2 cells. Two α-chaconine/α-solanine ratios were chosen, 1.7:1, a ratio found in some wild-type potato varieties, and 28.8:1, a ratio that can be achieved by genetic modification using a SGT1 anti-sense construct (*20*). The diverse glycoalkaloid treatments resulted in membrane disruptive activities of varying severity as determined by the cellular leakage of lactate dehydrogenase. This outcome was used as an anchor to assess the usefulness of DNA microarrays in screening for potential toxicities and the severity of these compounds alone and as mixtures.

2. MATERIALS AND METHODS

2.1. Biochemicals. α-Chaconine, α-solanine, and propidium iodide were obtained from Sigma Aldrich (St Louis, MO). Stock solutions of the glycoalkaloids and glycoalkaloid mixtures were prepared in dimethyl formamide (DMF) (Merck, Germany). The stock solutions were diluted with Dulbecco's modified Eagle's medium (DMEM) to the final desired concentrations immediately before use. In every experiment, cells in the control group were treated with an equivalent concentration of the solvent DMF (0.0005%, v/v).

2.2. Caco-2 Cell Culture. The human intestinal epithelial cell line Caco-2 (ATCC, Manassas, VA) was grown routinely in 75 cm^2 culture flasks at 37 °C in air with 5% CO_2 and 100% relative humidity in DMEM (BioWhittaker, Verviers, Belgium) supplemented with $NaHCO_3$ (3.7 g/L, Sigma), non-essential amino acids (1× NEAA; ICN, Zoetermeer, The Netherlands), fetal calf serum (FCS; 10%, v/v; Invitrogen, Breda, The Netherlands), penicillin (5000 units, Sigma), and streptomycin (5 mg/L, Sigma).

2.3. Lactate Dehydrogenase (LDH) Assay. A LDH assay was performed to assess the cytotoxic properties of α-chaconine, α-solanine, and two different glycoalkaloid mixtures. This assay detects the leakage of LDH from impaired cell membranes, which can be used as a measure of cytotoxcity. Caco-2 cells were seeded in 24-well plates (Costar) and grown for 19 days, allowing the cells to differentiate. Subsequently, the differentiated cells were exposed in quadruple for either 6 or 24 h to 5, 10, 15, and 20 μM α-chaconine ($n = 4$), α-solanine ($n = 4$), α-chaconine/α-solanine (1.7:1) ($n = 4$), and α-chaconine/α-solanine (28.8:1) ($n = 4$). LDH activity was determined using a CytoTox 96 nonradioactive cytotoxicity assay kit (Promega, Benelux bv, The Netherlands) in accordance with the instructions of the manufacturer.

2.4. Gene Expression Experiments. In three independent experiments, Caco-2 cells were seeded at a density of 40 000 per cm^2 in 6-well polyester Transwell plates (Costar; 0.4 μm pore size, inserts of 24 mm in diameter). The cells were allowed to differentiate by growing them for 19 days. Following differentiation, cells were exposed for 6 h to 10 μM of the following glycoalkaloid preparations: α-chaconine, α-solanine, α-chaconine/α-solanine (1.7:1), and α-chaconine/α-solanine (28.8:1). The exposure time and concentration were based on results from a previous study, in which optimal conditions for studying the effect of α-chaconine on gene expression were determined systematically (*23*). The media in the upper compartments of the transwells were

replaced with DMEM containing 0.01% DMF (control exposure) or one of the glycoalkaloid-containing solutions described above. The media in the lower compartments were replaced with DMEM only, to mimic conditions in the body.

After exposure, media were removed and both compartments were washed twice with ice-cold phosphate-buffered saline (PBS). Cells in the upper compartments were resuspended in 1 mL TriZol (Invitrogen, Breda, The Netherlands) and stored at −80 °C until RNA extraction.

2.5. Microarray Hybridizations. Total RNA from Caco-2 cells was isolated using the TriZol reagent according to the instructions of the manufacturer. RNA purification was performed using the RNeasy kit (Qiagen, Westburg bv, Leusden, The Netherlands). RNA integrity was verified by gel electrophoresis, and RNA concentrations and purity were determined by UV spectrometry by measuring 260/280 and 260/230 nm absorbance ratios, respectively. All RNA samples had $OD_{260/280}$ ratios between 1.9–2.1 and $OD_{260/230}$ ratios higher than 1.7.

A control reference design was used to analyze differential gene expression in glycoalkaloid-treated samples versus controls. RNA samples (2 μg each) were amplified and labeled with Cy5- and Cy3-CTP (PerkinElmer/NEN Life Sciences, Boston, MA) to produce labeled cRNA using Agilent low RNA input fluorescent linear amplification kits following the protocol of the manufacturer. For hybridization, the Agilent 60-mer oligo microarray processing protocol (Rev. 7, SSPE Wash/6-screw hybridization chamber) was followed. Briefly, 1 μg of Cy3-labeled control (reference sample) and 1 μg of Cy5-labeled glycoalkaloid-treatment sample were mixed and hybridized to a 22K 60-mer oligonucleotide Agilent human 1A oligo microarrays V2 (Agilent Technologies, Palo Alto, CA) for 17 h at 60 °C. Upon hybridization, the microarrays were washed and dried at room temperature following instructions by Agilent.

Arrays were scanned using a Scanner Array Express HT microarray scanner (PerkinElmer Life Sciences, Boston, MA). The software package, Array Vision Software 7.0 (Imaging Research, Ontario, Canada), was used to extract data from the scanned images. The quality of the arrays was checked by using Microsoft Excel 2000 (Microsoft Corporation, Redmond, WA) and the software package LimmaGUI in R version 2.3.1 (http://bioinf.wehi.edu.au/limmaGUI/index.html). Single spots or blemished areas on the array were flagged. The non-flagged fluorescence signals that were quantified using Array Vision software were exported to GeneMaths XT software (version 1.5, Applied Maths, St Martens-Latem, Belgium) for further analyses. Array elements for which the fluorescent intensity in each channel was less than 1.5 times the background were excluded, leaving 10 829 transcripts for subsequent analyses. Data normalization was performed with GeneMaths XT, as described previously (*23*).

2.6. Data Analysis. Identification of genes differentially expressed between a glycoalkaloid treatment and control group was performed by using both an unpaired Student's *t* test with p value < 0.01 or < 0.001 and a fold change criterion > 1.5.

Two complementary methods were applied to relate changes in gene expression to functional changes. First, an online software suite MetaCore version 4.3 (GeneGo, Inc., St. Joseph, MI) was used to identify statistically significant pathways responding to the different glycoalkaloid treatments. For this purpose, only the data of genes found to be significantly differentially expressed ($p < 0.01$ and fold change > 1.5) were imported into the MetaCore program. MetaCore analyses resulted in lists of maps/pathways ranked according to significance (lowest p values), as outlined by Ekins et al. (*24*).

The other approach used was based on over-representation of gene ontology (GO) terms. The software package ErmineJ (*25*), which uses a scoring-based resampling method, was applied to identify significant enrichment or over-representation of biological processes responding to specific glycoalkaloid treatments. All *t*-test p values from the probe set comparisons across each glycoalkaloid treatment, and control groups were used for these analyses.

A one-way analysis of variance (ANOVA) test ($p < 0.001$) was performed in GeneMaths XT to determine genes that were differentially expressed across the glycoalkaloid treatments. Principal component analysis (PCA) and hierarchical clustering analyses were performed in GeneMaths XT. The gene subset that was identified to be differentially expressed following ANOVA analysis was used for those analyses. Pearson correlation and the unweighted pair group method with arithmetic means (UPGMA) were used to determine the clustering of experimental groups.

2.7. Cell-Cycle Analysis. Cell-cycle analysis was performed on Caco-2 cells grown for 19 days in 6-well polyester Transwell plates exposed to 5, 10, and 20 μM α-chaconine ($n = 3$) for 6 or 24 h. Caco-2 cells were harvested with trypsin, washed twice with cold PBS, and then resuspended in cold PBS. Cells subsequently were fixed in 70% ethanol for 30 min and stored at 4 °C. Before processing, cells were collected by centrifugation and incubated in RNase (1 mg/mL) for 30 min at 37 °C. Propidium iodide (100 μg/mL) was added, and samples were incubated for 30 min at room temperature. Cell-cycle analysis was performed using a FACSarray flow cytometer (Becton Dickinson, San Jose, CA). In each experiment, a minimum of 20 000 events were evaluated. Cell-cycle distribution was analyzed using FACSdiva software (Becton Dickinson, San Jose, CA). To identify the significant difference between each experimental test condition and control treatment, a Student's *t* test was performed. A p value < 0.05 was regarded as indicating statistical significance.

2.8. Determination of Apoptosis. The Annexin V assay was conducted on Caco-2 cells grown for 19 days in 6-well polyester Transwell plates exposed to 5, 10, and 20 μM α-chaconine ($n = 4$) for 6 h. When apoptosis is initiated, the lipid organization of the plasma membrane is altered, exposing phosphatidylserine on the outer membrane surface. Annexin V was used to detect exposure of phosphatidylserine, because it is one of the markers for the early stage of apoptosis (*26*). Cells were harvested with trypsin, washed twice in cold PBS, and resuspended in binding buffer. The cells were washed and subsequently incubated with 2 μL of Annexin V-Fluos (Roche Diagnostics, Penzberg, Germany) in 200 μL of Annexin V buffer according to the protocol of the manufacturer. After an incubation period of 15 min at room temperature, the cells were spun-down and resuspended in 200 μL of Annexin V buffer and 2 μL of propidium iodide (PI; 1 mg/mL; Sigma). The cells were then immediately analyzed on a FACSArray flow cytometer (Becton Dickinson, San Jose, CA). In each experiment, a minimum of 10 000 events were evaluated. Cell death was analyzed using FACSDiva software (Becton Dickinson, San Jose, CA). A Student's *t* test was performed to identify the significant difference between each experimental test condition and control treatment. A p value < 0.05 was regarded as indicating statistical significance.

3. RESULTS

3.1. LDH Leakage. Exposure of differentiated Caco-2 cells to increasing concentrations of glycoalkaloid treatments for 6 or 24 h resulted in concentration-dependent leakage of LDH at both time points (**Figure 2**). For all treatments, except α-solanine alone, the higher glycoalkaloid concentration of 20 μM resulted in LDH leakage of more than 20% after 6 and 24 h of exposure. This latter level is used frequently as a lower cutoff for cytotoxicity. With respect to the 10 μM exposures, only the α-chaconine/α-solanine mixture (1.7:1) resulted in a LDH leakage greater than 20% at both exposure times.

The extent of LDH leakage was comparable at 6 and 24 h when cells were treated with α-chaconine alone or the mixture of α-chaconine/α-solanine (28.8:1) (**Figure 2**). α-Solanine, when administered alone for 24 h, caused relatively less membrane disruption, irrespective of the concentration. In general, glycoalkaloid exposures for 24 h induced LDH leakage with the following order of potency: α-chaconine/α-solanine (1.7:1) > α-chaconine/α-solanine (28.8:1) = α-chaconine > α-solanine at all concentrations of exposure. After 6 h of exposure, α-solanine caused less disruption at 20 μM, whereas at concentrations of 15 μM or less, the degree of LDH leakage was similar to that observed when cells were treated with α-chaconine alone or with α-chaconine/α-solanine (28.8:1).

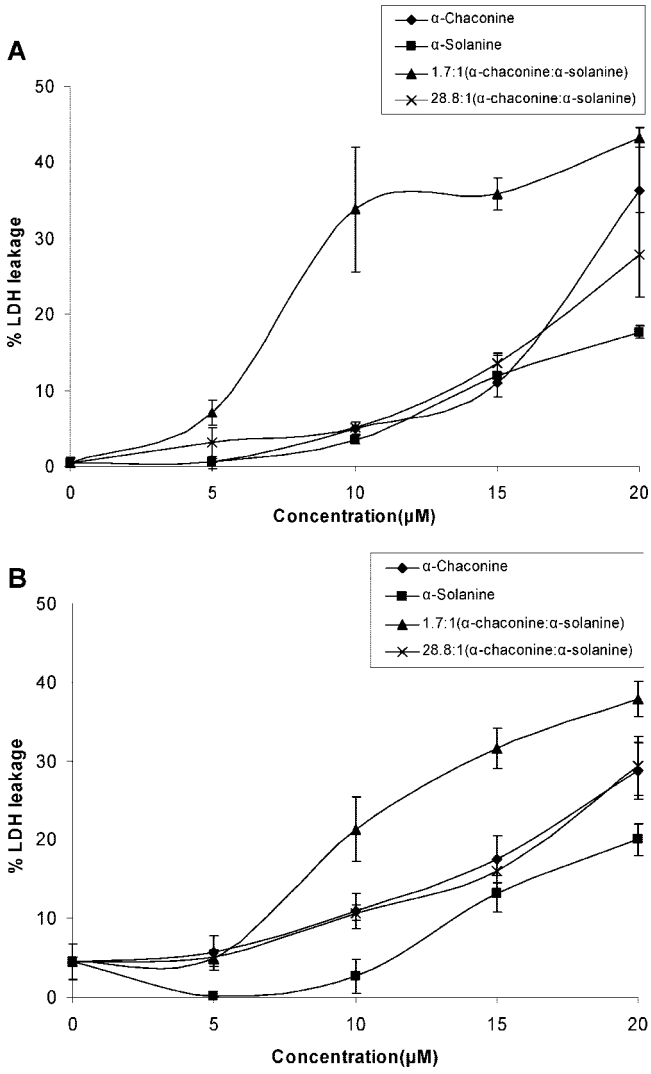

Figure 2. Concentration-dependent LDH leakage induced by the glycoalkaloid treatments after (**A**) 6 h and (**B**) 24 h exposures. Each point represents the average of four replicates, with a standard deviation of less than 5%.

3.2. Gene Expression Studies: Exposure of Caco-2 Cells to α-Solanine, α-Chaconine, and Glycoalkaloid Mixtures. Gene expression profiles were determined to assess glycoalkaloid-induced transcriptional effects. The number of genes up- or downregulated at significance levels of either $p < 0.01$ or < 0.001 and that exhibited fold changes > 1.5 are shown in **Table 1**. α-Solanine (10 μM) had very little effect on gene expression in the Caco-2 cell line compared to the other treatments that were tested.

PCA and hierarchical clustering analyses were performed using 444 genes that were expressed differentially by at least one of the glycoalkaloid treatments (ANOVA, $p < 0.001$). These results were consistent with a compound-specific response on gene expression (**Figure 3**). Cells exposed to α-solanine alone were clustered closer to control cells. The other glycoalkaloid treatments elicited markedly distinct gene expression profiles from those of the control and α-solanine-only groups. Gene-expression profiles observed following α-chaconine and α-chaconine/α-solanine (28.8:1) treatments were more similar to each other than to the profile observed following α-chaconine/α-solanine (1.7:1) treatment.

Genes differentially expressed following distinct glycoalkaloid treatments ($p < 0.01$ and fold changes > 1.5) were imported into MetaCore to identify pathways that were affected by the respective treatments. Microarray data obtained with α-solanine were not subjected to MetaCore analysis because only seven genes were differentially expressed following this treatment. The 10 most significantly affected pathways by the various treatments tested that were identified by MetaCore are presented in **Table 2**.

Comparisons of treatment effects on Caco-2 cell gene expression revealed that cholesterol biosynthesis was one of the pathways most significantly affected by both α-chaconine administered alone and the α-chaconine/α-solanine (28.8:1) mixture (**Table 2**). These treatments resulted in the upregulation of several genes involved in cholesterol biosynthesis ($p < 0.01$ and fold change > 1.5) (**Table 4**). The α-chaconine/α-solanine (1.7:1) mixture did not significantly affect the cholesterol biosynthesis pathway (**Table 2**). Most importantly, the rate-limiting enzyme of cholesterol biosynthesis, 3-hydroxy-3-methylglutaryl-coenzyme A reductase (HMGCR), was not significantly induced by α-chaconine/α-solanine (1.7:1) (**Table 4**).

Generally, MetaCore analysis revealed that the glycoalkaloid treatments affected the same pathways and genes. Besides cholesterol biosynthesis, most of the pathways affected appeared to be those involved in growth-related signaling (e.g., EGF), lipid metabolism, transcription regulation of amino acid metabolism, Ras family GTPases cascades, and chemokine- and cytokine-mediated signaling.

A parallel analysis using ErmineJ was performed to determine the biological processes affected by the different glycoalkaloid treatments. These results were consistent with those obtained by MetaCore (**Table 3**). For all glycoalkaloid treatments, similar processes were found to be affected. Over-represented GO classes included descriptors for lipid metabolism, cytokine- and chemokine-mediated pathways, amino acid metabolism, MAPK and NF-κB cascades, cell death/apoptosis, and the cell cycle. As found with MetaCore analysis, cholesterol biosynthesis was observed to be affected significantly by α-chaconine and α-chaconine/α-solanine (28.8:1) exposure and not by α-chaconine/α-solanine (1.7:1). More cell death/apoptotic and oxidative stress processes were regulated differentially by this latter treatment.

In a dose–response microarray experiment conducted with these glycoalkaloid treatments, induction of cholesterol biosynthesis genes was evident at low concentrations of 5 μM glycoalkaloid (mixtures), except when α-solanine was administered alone (data not shown). Cholesterol biosynthesis genes were only induced at a concentration of 20 μM following this latter treatment. Except for α-solanine administered alone, glycoalkaloid concentrations of 20 μM affected apoptotic/cell death pathways rather than the cholesterol biosynthesis pathway (data not shown). **Table 4** presents lists of genes classified in selected processes that were affected by the specified treatments.

3.2.3. Cell-Cycle Analysis. Gene-expression analyses revealed that cell-cycle genes were also affected significantly by the glycoalkaloid treatments (**Table 4**). Therefore, a cell-cycle analysis was performed to determine which cell-cycle phase(s) was affected. In general, an accumulation of cells in the G_2/M phase was noted after 6 or 24 h of exposure to 5, 10, or 20 μM α-chaconine (**Figure 4**).

3.2.4. Determination of Apoptosis. Our data revealed a concentration-dependent increase in a late apoptotic or necrotic phase in Caco-2 cells exposed to 5, 10, and 20 μM α-chaconine

Table 1. Numbers of Significantly Up- and Downregulated Genes in Caco-2 Cells after Treatment with Glycoalkaloids[a]

	$p \leq 0.01$ (FC ≥ 1.5)			$p \leq 0.001$ (FC ≥ 1.5)		
glycoalkaloid treatment	upregulated	downregulated	total	upregulated	downregulated	total
10 μM α-solanine	2	5	7	–	–	–
10 μM α-chaconine	354	97	451	124	20	144
10 μM α-chaconine/α-solanine (28.8:1)	310	204	514	97	27	124
10 μM α-chaconine/α-solanine (1.7:1)	264	157	421	50	15	65

[a] FC, fold change; *p*, Student's *t*-test *p* value; –, no differentially expressed genes found.

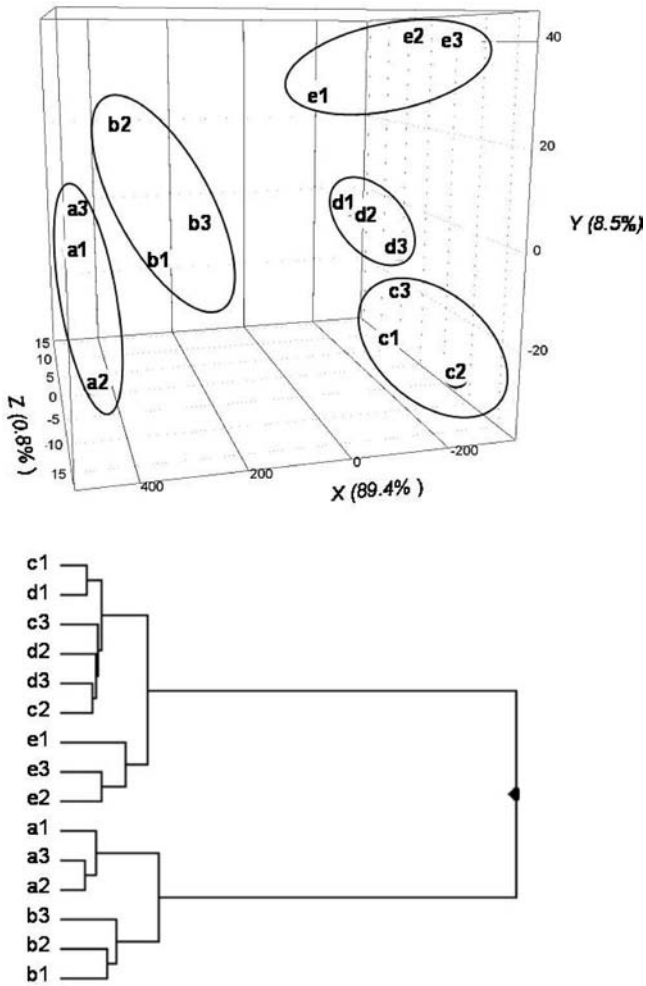

Figure 3. PCA mapping and hierarchical clustering of the different glycoalkaloid treatments with genes found to be significantly differentially expressed (ANOVA, $p \leq 0.001$). The axes on the PCA plot show the gene-expression profiles of the different treatment groups in the principal component *x*, *y*, and *z* (which explain the largest part of the variance). a, control cells; b, cells exposed to α-solanine; c, cells exposed to α-chaconine; d, cells exposed to α-chaconine/α-solanine (28.8:1); and e, cells exposed to α-chaconine/α-solanine (1.7:1). The results are based on three (1–3) independent experiments.

for 6 h. We did not observe any significant effect on the early apoptotic cells at the concentrations tested (**Figure 5**).

DISCUSSION

The toxic effects of single and mixtures of potato glycoalkaloids on gene expression in Caco-2 cells were investigated, and the utility of DNA microarrays in screening for toxic effects, assessing effect severity, and identifying potential mechanisms of toxicity were evaluated in this model system. Differences in the responses to the various glycoalkaloid treatments were mainly due to the differing degrees of potency of the glycoalkaloids, as noted in earlier studies (*4, 5, 18*). DNA microarrays, to varying extents, discriminated severity of effect/potency among the different glycoalkaloid treatments.

α-Solanine (10 μM) was the least potent of the glycoalkaloid treatments, as observed in both LDH leakage and gene profiling experiments. α-Solanine administered alone caused less LDH leakage compared to equimolar amounts of α-chaconine and the glycoalkaloid mixtures. PCA and hierarchical cluster analyses revealed that the gene expression profile of cells treated with 10 μM α-solanine mostly resembled that of control cells, but expression profiles of cells subjected to the other glycoalkaloid treatments differed significantly from those of the controls. α-Chaconine alone (10 μM) and α-chaconine/α-solanine (28.8:1, 10 μM) had similar gene expression profiles in Caco-2 cells, suggesting common mechanisms of action and/or similar degrees of effect. In addition, these latter treatments resulted in similar LDH leakage. On the other hand, exposure to 10 μM α-chaconine/α-solanine (1.7:1) resulted in a gene expression profile that was distinguishable from those observed following the other treatments. As documented by LDH leakage experiments, 10 μM α-chaconine/α-solanine (1.7:1) was the most potent membrane disrupter. Clearly, glycoalkaloid treatments elicited signature patterns of gene expression that appeared to reflect potency, thereby indicating the usefulness of DNA microarrays to screen for differences in potencies of distinct glycoalkaloid treatments and, as is described below, provide additional valuable information.

To obtain a comprehensive overview of the response of Caco-2 cells to the selected glycoalkaloid treatments that were tested, significant over-representation of differentially expressed genes with roles in specific biological processes and pathways were identified using ErmineJ and MetaCore, respectively. Those analyses revealed that, for the most part, similar biological processes/pathways were affected by the tested treatments. Pathways/biological processes affected by all of the tested treatments included cytokine- and chemokine-mediated signaling, growth signaling, MAPK and NF-κB cascades, lipid metabolism, the cell cycle, and cell death/apoptosis. The most distinctive observation was the significant induction of the cholesterol biosynthesis pathway in Caco-2 cells by either α-chaconine/α-solanine (28.8:1) or α-chaconine alone but not by the other treatments.

Intestinal membrane disruptive activity is the most well-described toxic mechanism of action of the potato glycoalkaloids. Those effects were attributed to the formation of destabilizing complexes between the lipophilic moieties of glycoalkaloids and membrane-bound cholesterol (*27–29*). In previous work, we observed that α-chaconine induced cholesterol biosynthesis genes in Caco-2 cells prior to other changes reflective of cytotoxicity. This pathway ceased to be important with either prolonged exposure to low α-chaconine concentrations or shorter exposure to higher, cytotoxic concentrations of

Table 2. Top 10 Lists of MetaCore Pathways Affected by the Glycoalkaloid Treatments

number	map	*p* value[a]	expressed[b]	all[c]
	10 μM α-Chaconine			
1	cholesterol biosynthesis	4.592×10^{-10}	9	21
2	EGF-signaling pathway	1.764×10^{-5}	9	64
3	EGFR signaling via small GTPases	3.037×10^{-5}	7	39
4	transcription regulation of amino acid metabolism	4.263×10^{-5}	7	41
5	oncostatin M signaling via MAPK in mouse cells	5.013×10^{-5}	7	42
6	oncostatin M signaling via MAPK in human cells	5.868×10^{-5}	7	43
7	VEGF signaling via VEGFR2, generic cascades	6.839×10^{-5}	7	44
8	IGF–RI signaling	0.000 280 9	8	72
9	MIF in innate immunity response	0.000 325 1	7	56
10	AKT signaling	0.000 363 2	7	57
	10 μM α-Chaconine/α-Solanine (28.8:1)			
1	transcription regulation of amino acid metabolism	1.356×10^{-5}	8	41
2	cholesterol biosynthesis	1.632×10^{-5}	6	21
3	oncostatin M signaling via MAPK in mouse cells	0.005 757	5	42
4	role of AP-1 in regulation of cellular metabolism	0.006 37	5	43
5	oncostatin M signaling via MAPK in human cells	0.006 37	5	43
6	Ras family GTPases in kinase cascades (scheme)	0.006 946	4	28
7	VEGF signaling via VEGFR2, generic cascades	0.007 027	5	44
8	triacylglycerol metabolism p.1	0.007 885	4	29
9	EGF signaling pathway	0.008 32	6	64
10	IL2 activation and signaling pathway	0.008 481	5	46
	10 μM α-Chaconine/α-Solanine (1.7:1)			
1	phospholipid metabolism p.2	0.001 715	3	11
2	EGF-signaling pathway	0.003 392	6	64
3	PPAR regulation of lipid metabolism	0.003 588	4	28
4	fatty acid omega oxidation	0.003 596	3	14
5	triacylglycerol metabolism p.1	0.004 088	4	29
6	proline metabolism	0.004 42	3	15
7	methionine–cysteine–glutamate metabolism	0.007 534	3	18
8	role of VDR in regulation of genes involved in osteoporosis	0.009 688	5	57
9	transcription regulation of amino acid metabolism	0.014 07	4	41
10	P53-signaling pathway	0.020 75	4	46

[a] For a calculation of *p* values, see the Materials and Methods. [b] The number of differentially expressed genes ($p < 0.01$ and FC > 1.5) in a pathway/map. [c] The total number of genes in a particular pathway/map.

α-chaconine (*23*). Therefore, it is likely that disturbances in cellular cholesterol levels/homeostasis as a result of the formation of membrane glycoalkaloid/sterol complexes result in the induction of cholesterol biosynthesis to regain homeostasis. We also observed general downregulation of lipid metabolism pathways that use cholesterol (e.g., decreased expression of SULT2A1 and UGT2B7 involved in steroid metabolism, **Table 4**), and as such, influence intracellular cholesterol levels might be explained in this view.

Results of both MetaCore and ErmineJ analyses indicated that non-cytotoxic concentrations (LDH leakage < 20%) of 10 μM of either α-chaconine alone or the α-chaconine/α-solanine (28.8:1) mixture induced genes of the cholesterol biosynthesis pathway. In contrast, α-chaconine/α-solanine (1.7:1) did not significantly affect the cholesterol biosynthesis pathway. The results from the LDH assay suggest that α-chaconine and α-solanine act synergistically when present in the ratio of 1.7:1 and that this mixture is more potent than equivalent concentrations of either α-chaconine or α-solanine alone. We suggest that the induction of cholesterol biosynthesis is precluded by apoptotic processes that result in cell death. Other studies have also shown that, at certain α-chaconine/α-solanine ratios, mixtures of glycoalkaloids interact synergistically, resulting in increased toxicity (*5, 13, 16–18*).

Exposure to α-chaconine was shown to result in greater membrane disruptive effects than exposure to α-solanine (*4, 5, 18*). The differences in potency between α-solanine and α-chaconine can either be explained by subtle changes in the sugar moiety volume or by the different side chains on the sugar ring structures that influence sugar–sugar intermolecular interactions and, thereby, the formation of stable glycoalkaloid–sterol complexes (*27*). α-Solanine binds to membrane-bound cholesterol but to a lesser extent than α-chaconine, thus resulting in reduced membrane disruption compared to that observed following α-chaconine exposure (*5*). A concentration of 10 μM α-solanine proved to be too low to detect any effects on gene expression. Exposure of Caco-2 cells to 20 μM α-solanine (data not shown) affected the same pathways as did exposure to 5 or 10 μM α-chaconine and to α-chaconine/α-solanine mixtures, indicating similarities in their mechanisms of action. For example, the induction of cholesterol biosynthesis genes by α-solanine was only observed at a higher concentration of 20 μM and not at 10 μM.

Because several cell-cycle genes were affected by the treatments, cell-cycle analysis experiments were conducted using α-chaconine. Yang et al. (*30*) showed that the exposure of intestinal HT29 cells to 5 μg/mL (~5.9 μM) α-chaconine and 10 μg/mL (~11.5 μM) α-solanine for more than 48 h induced accumulation of cells in the sub-G_0/G_1 phase. However, our data indicated accumulation of Caco-2 cells in the G_2/M phase at concentrations of 5–20 μM. We also exposed cells to 100 μM α-chaconine (6/24 h) (data not shown); however, we were unable to measure 20 000 events because of significant cell death. Despite this, it appears that cells tend to accumulate disproportionately in the G_0/G_1 phase when exposed to higher glycoalkaloid concentrations. These results imply that the effect of α-chaconine on the cell cycle may depend upon the cell type and/or exposure concentration. Among the cell-cycle genes affected by all of the selected treatments in the current study was polo kinase 3 (Plk3), which is involved in the regulation

Table 3. Gene Ontology Classes Over-represented following Glycoalkaloid Treatment[a]

number	GO class	GO ID	probes	genes in class	raw score	FDR
		10 μM α-Chaconine				
1	cell-substrate adhesion	GO:0031589	24	23	1.43	5.21×10^{-10}
2	protein targeting	GO:0006605	59	54	1.15	2.61×10^{-10}
3	epidermis development	GO:0008544	32	32	1.49	1.74×10^{-10}
4	protein amino acid dephosphorylation	GO:0006470	66	61	1.19	1.30×10^{-10}
5	cell death	GO:0008219	18	17	1.53	1.04×10^{-10}
6	locomotion	GO:0040011	64	57	1.09	8.68×10^{-11}
7	protein amino acid O-linked glycosylation	GO:0006493	16	15	2.68	7.44×10^{-11}
8	anti-apoptosis	GO:0006916	67	63	1.17	6.51×10^{-11}
9	main pathways of carbohydrate metabolism	GO:0006092	73	66	1.07	5.79×10^{-11}
10	cholesterol biosynthesis	GO:0006695	23	18	2.18	5.21×10^{-11}
11	glycerol metabolism	GO:0006071	9	9	2.87	4.74×10^{-11}
12	actin cytoskeleton organization and biogenesis	GO:0030036	61	55	1.39	4.34×10^{-11}
13	dephosphorylation	GO:0016311	68	63	1.18	4.01×10^{-11}
14	cell migration	GO:0016477	32	29	1.47	3.72×10^{-11}
15	regulation of translation	GO:0006445	59	56	1.34	3.47×10^{-11}
16	positive regulation of I-κB kinase/NF-κB cascade	GO:0043123	51	48	1.66	3.26×10^{-11}
17	microtubule-based movement	GO:0007018	40	38	1.49	3.07×10^{-11}
18	vesicle-mediated transport	GO:0016192	118	110	0.90	2.89×10^{-11}
19	cytokine- and chemokine-mediated signaling pathway	GO:0019221	12	10	3.65	2.74×10^{-11}
20	response to virus	GO:0009615	30	30	1.52	2.61×10^{-11}
		10 μM α-Chaconine/α-Solanine (28.8:1)				
1	epidermis development	GO:0008544	32	32	2.06	5.21×10^{-10}
2	protein amino acid dephosphorylation	GO:0006470	66	61	1.36	2.61×10^{-10}
3	translational elongation	GO:0006414	15	13	1.96	1.74×10^{-10}
4	cell death	GO:0008219	18	17	2.39	1.30×10^{-10}
5	protein amino acid O-linked glycosylation	GO:0006493	16	15	1.78	1.04×10^{-10}
6	anti-apoptosis	GO:0006916	67	63	1.61	8.68×10^{-11}
7	inactivation of MAPK activity	GO:0000188	11	11	2.12	7.44×10^{-11}
8	cholesterol biosynthesis	GO:0006695	23	18	2.68	6.51×10^{-11}
9	glycerol metabolism	GO:0006071	9	9	2.81	5.79×10^{-11}
10	dephosphorylation	GO:0016311	68	63	1.34	5.21×10^{-11}
11	cell migration	GO:0016477	32	29	1.47	4.74×10^{-11}
12	positive regulation of I-κB kinase/NF-κB cascade	GO:0043123	51	48	1.49	4.34×10^{-11}
13	organ development	GO:0048513	108	97	1.10	4.01×10^{-11}
14	microtubule-based movement	GO:0007018	40	38	1.66	3.72×10^{-11}
15	cytokine- and chemokine-mediated signaling pathway	GO:0019221	12	10	2.68	3.47×10^{-11}
16	response to virus	GO:0009615	30	30	1.55	3.26×10^{-11}
17	DNA catabolism	GO:0006308	9	9	2.65	3.07×10^{-11}
18	Golgi vesicle transport	GO:0048193	81	73	1.11	2.89×10^{-11}
19	DNA replication	GO:0006260	89	84	1.32	2.74×10^{-11}
20	hemopoiesis	GO:0030097	12	11	4.76	2.61×10^{-11}
		10 μM α-Chaconine/α-Solanine (1.7:1)				
1	main pathways of carbohydrate metabolism	GO:0006092	73	66	1.19	5.21×10^{-10}
2	integrin-mediated signaling pathway	GO:0007229	30	26	2.01	2.61×10^{-10}
3	negative regulation of programmed cell death	GO:0043069	12	11	2.39	1.74×10^{-10}
4	positive regulation of I-κB kinase/NF-κB cascade	GO:0043123	51	48	1.49	1.30×10^{-10}
5	DNA integrity checkpoint	GO:0031570	9	8	3.02	1.04×10^{-10}
6	positive regulation of MAPK activity	GO:0043406	10	9	2.27	8.68×10^{-11}
7	cytokine- and chemokine-mediated signaling pathway	GO:0019221	12	10	2.37	7.44×10^{-11}
8	DNA catabolism	GO:0006308	9	9	3.91	6.51×10^{-11}
9	positive regulation of signal transduction	GO:0009967	59	53	1.65	5.79×10^{-11}
10	death	GO:0016265	13	12	1.95	5.21×10^{-11}
11	G2/M transition of mitotic cell cycle	GO:0000086	12	9	2.57	4.74×10^{-11}
12	apoptotic nuclear changes	GO:0030262	9	8	2.68	4.34×10^{-11}
13	oxygen and reactive oxygen species metabolism	GO:0006800	37	36	1.40	4.01×10^{-11}
14	physiological interaction between organisms	GO:0051706	17	14	3.12	3.72×10^{-11}
15	DNA damage response, signal transduction	GO:0042770	13	12	2.01	3.47×10^{-11}
16	prostaglandin metabolism	GO:0006693	9	9	2.39	3.26×10^{-11}
17	response to oxidative stress	GO:0006979	34	33	1.54	3.07×10^{-11}
18	cellular lipid metabolism	GO:0044255	85	79	1.24	2.89×10^{-11}
19	cellular macromolecule catabolism	GO:0044265	13	12	1.97	2.74×10^{-11}
20	response to chemical stimulus	GO:0042221	108	104	1.13	2.61×10^{-11}

[a] A scoring-based resampling method was used to identify significantly over-represented GO classes. More than 10 000 *t*-test *p* values from the probe set comparisons across the glycoalkaloid treatments were used. The analysis was performed using the tool ErmineJ (*23*). Only classes for the concept "biological process" (top 20 with a FDR < 0.0001) are shown. For the analysis, only classes containing 8–125 genes were taken into account.

of cell-cycle progression through the M phase (*31*). Plk3 is a NF-κB downstream target gene (*32*) and induces cell death, possibly by inducing p53-dependent and -independent pathways. Ectopic expression of Plk3 or its mutants perturbs microtubule integrity, resulting in dramatic morphological changes, G_2/M arrest, and apoptosis (*31*). Also induced in the present experiments was cyclin-dependent kinase inhibitor 1A (CDKN1A or p21 or Cip1), which inhibits both cyclin-dependent G_1 kinases (*33*) and the G_2/M-specific cdc2 kinase (*34*–*36*). Thus, CDKN1A can result in cell-cycle arrest in either the G_1 or G_2/M phase. Also

Table 4. Partial List of Differentially Expressed Genes Classified According to Selected Processes Commonly Affected by All Treatments[a]

		10 μM α-solanine		10 μM α-chaconine		10 μM GA mixture (28.8:1)		10 μM GA mixture (1.7:1)	
gene name	gene ID	FC	*p* value	FC	*p* value	FC	*p* value	FC	*p* value
Cholesterol/Sterol Biosynthesis									
3-hydroxy-3-methylglutaryl-coenzyme A reductase (HMGCR)	NM_000859	1.19	0.462 013	3.53	0.000 638	2.46	0.000 747	1.08	0.339 773
3-hydroxy-3-methylglutaryl-coenzyme A synthase 1 (soluble) (HMGCS1)	NM_002130	1.61	0.046 436	3.47	0.001 317	3.42	0.000 248	2.02	0.024 735
cytochrome P450, family 51, subfamily A, polypeptide 1 (CYP51A1)	NM_000786	1.29	0.117 001	2.03	0.000 333	1.84	0.000 212	1.21	0.050 832
squalene epoxidase (SQLE)	NM_003129	1.30	0.098 264	3.14	0.000 889	2.91	0.008 428	1.72	0.035 499
sterol-C5-desaturase (ERG3 δ-5-desaturase homologue, fungal)-like (SC5DL)	NM_006918	1.23	0.253 956	2.21	0.007 952	2.10	0.003 434	1.37	0.043 46
sterol-C5-desaturase (ERG3 δ-5-desaturase homologue, fungal)-like, (cDNA clone MGC:2084 MAGE:3537285)	BC012333	1.20	0.191 643	2.55	0.001 105	2.41	0.001 199	1.42	0.026 284
sterol-C4-methyl oxidase-like (SC4MOL)	NM_006745	1.46	0.035 287	2.04	0.000 714	1.90	0.000 229	1.38	0.133 572
mevalonate kinase (mevalonic aciduria) (MVK)	NM_000431	1.07	0.805 267	1.71	0.002 905	1.51	0.038 069	0.73	0.023 069
Homo sapiens /hepatitis B virus fusion for mevalonate kinase	X75311	0.97	0.916 08	1.76	0.0329	1.57	0.105 179	0.85	0.457 067
sterol regulatory element binding transcription factor 1 (SREBF1), transcript variant 2	NM_004176	1.06	0.816 728	1.65	0.001 823	1.48	0.069 865	1.44	0.059 699
sterol regulatory element binding transcription factor 2 (SREBF2)	NM_004599	1.08	0.294 725	1.48	0.003 126	1.28	0.012 238	1.11	0.116 347
farnesyl diphosphate synthase (farnesyl pyrophosphate synthetase) (FDPS)	NM_002004	1.23	0.217 881	1.75	0.002 132	1.42	0.029 285	1.06	0.527 974
farnesyl-diphosphate farnesyltransferase 1 (FDFT1)	NM_004462	1.13	0.535 23	2.25	0.000 949	1.74	0.024 414	1.05	0.554 356
acetyl-coenzyme A acetyltransferase 2 (acetoacetyl coenzyme A thiolase) (ACAT2)	NM_005891	1.08	0.818 932	1.82	0.002 172	1.41	0.032 83	0.99	0.918 362
low-density lipoprotein receptor (familial hypercholesterolemia) (LDLR)	NM_000527	1.44	0.128 684	3.63	0.000 499	3.33	0.007 036	2.30	0.007 428
isopentyl disphosphate isomerase (IDI1)	NM_004508	1.13	0.622 388	2.89	6.40×10^{-5}	2.59	0.000 436	1.44	0.050 39
Lipid Metabolism									
likely orthologue of mouse acyl-coenzyme A thioesterase 2, mitochondrial (ACATE2)	NM_012332	1.12	0.370 984	2.26	6.30×10^{-5}	1.95	0.001 83	1.73	0.000 397
dihydrolipoamide *S*-acetyltransferase (E2 component of pyruvate dehydrogenase complex) (DLAT)	NM_001931	1.01	0.841 188	1.46	0.000 213	1.21	0.013 567	1.06	0.297 008
cytochrome P450, family 3, subfamily A, polypeptide 5 (CYP3A5)	NM_000777	1.16	0.017 193	1.22	0.003 768	1.32	0.000 391	1.37	0.000 301
malonyl-CoA decarboxylase (MLYCD)	NM_012213	0.89	0.197 086	0.59	0.002 579	0.54	0.004 72	0.68	0.007 64
phosphatidylcholine transfer protein (PCTP)	NM_021213	0.91	0.286 463	0.75	0.011 503	0.64	0.001 818	0.63	0.001 254
nuclear receptor subfamily 2, group F, member 2 (NR2F2)	NM_021005	0.89	0.496 072	0.25	0.000 482	0.22	0.000 088	0.39	0.005 142
sulfotransferase family, cytosolic, 2A, dehydroepiandrosterone (DHEA)-preferring, member 1 (SULT2A1)	NM_003167	0.84	0.151 283	0.62	0.003 309	0.65	0.011 688	0.62	0.006 45
UDP glycosyltransferase 2 family, polypeptide B7 (UGT2B7)	NM_001074	0.74	0.043 648	0.62	0.008 049	0.61	0.018 008	0.58	0.007 79
acetyl-coenzyme A acyltransferase (ACAA1), nuclear gene encoding mitochondrial protein	NM_001607	0.81	0.119 165	0.72	0.102 146	0.60	0.001 572	0.55	0.001 403
choline kinase α (CHKA), transcript variant 1	NM_001277	1.18	0.050 329	1.45	0.042 749	1.54	0.027 971	1.57	0.002 661
fatty acid binding protein 5 (psoriasis-associated) (FABP5)	NM_001444	0.80	0.036 323	0.62	0.007 922	0.66	0.000 014	0.67	0.001 734
ferredoxin reductase (FDXR), nuclear gene encoding mitochondrial protein, transcript variant 2	NM_004110	0.84	0.090 416	0.88	0.213 827	0.77	0.136 108	0.64	0.003 278
monoglyceride lipase (MGLL), transcript variant 1	NM_007283	1.07	0.240 551	2.22	0.004 31	1.95	0.014 279	1.73	0.000 186
platelet-activating factor acetylhydrolase, isoform Ib, α subunit 45 kDa (PAFAH1B1)	NM_000430	1.06	0.410 604	1.60	0.004 101	1.66	0.007 962	1.58	0.003 005
Apoptosis/Programmed Cell Death									
B-cell CLL/lymphoma 10 (BCL10)	NM_003921	1.26	0.106 827	2.34	0.001 278	2.05	0.001 197	1.81	0.009 346
pleckstrin homology-like domain, family A, member 1 (PHLDA1)	NM_007350	1.58	0.034 105	3.30	0.000 334	3.81	0.000 079	4.03	0.002 348
pleckstrin homology-like domain, family A, member 2 (PHLDA2)	NM_003311	1.53	0.115 573	4.69	0.000 916	5.00	0.000 709	6.25	0.013 172
BCL2 binding component 3 (BBC3)	NM_014417	1.30	0.080 683	4.36	0.000 112	3.74	0.006 004	2.00	0.018 965
SH3-domain GRB2-like endophilin B1 (SH3GLB1)	NM_016009	1.12	0.100 532	1.94	0.000 195	1.90	0.000 861	1.54	0.002 113
tribbles homologue 3 (*Drosophila*) (TRIB3)	NM_021158	1.39	0.262 859	4.27	0.001 354	2.98	0.006 729	1.82	0.038 111
tumor necrosis factor receptor superfamily, member 1A (TNFRSF1A)	NM_001065	1.23	0.421 639	2.65	4.10×10^{-5}	2.04	0.001 448	1.86	0.000 36

Table 4. Continued

gene name	gene ID	10 μM α-solanine		10 μM α-chaconine		10 μM GA mixture (28.8:1)		10 μM GA mixture (1.7:1)	
		FC	*p* value	FC	*p* value	FC	*p* value	FC	*p* value
tumor necrosis factor receptor superfamily, member 12A (TNFRSF12A)	NM_016639	1.46	0.021 69	4.67	0.000 124	5.21	0.000 577	4.95	0.001 486
tumor necrosis factor receptor superfamily, member 21 (TNFRSF21)	NM_014452	1.38	0.041 717	2.38	0.001 824	2.09	0.002 007	1.88	0.011 591
kruppel-like factor 6 (KLF6), transcript variant 2	NM_001300	2.07	0.023 023	10.77	0.000 021	8.87	0.000 134	5.85	0.001 658
myeloid cell leukemia sequence 1 (BCL2-related) (MCL1), transcript variant 1	NM_021960	1.43	0.009 187	3.61	0.000 072	3.70	0.000 091	3.06	0.001 308
programmed cell death 8 (apoptosis-inducing factor) (PDCD8), nuclear gene encoding mitochondrial protein	NM_004208	0.68	0.019 167	0.64	0.014 379	0.59	0.007 481	0.55	0.003 852
extra spindle poles like 1 (*Saccharomyces cerevisiae*) (ESPL1)	NM_012291	0.90	0.306 476	0.63	0.003 176	0.59	0.001 181	0.64	0.005 335
Bcl2 modifying factor (BMF), transcript variant 2	NM_033503	0.90	0.424 475	0.63	0.010 225	0.57	0.008 203	0.52	0.018 726
Cell Cycle									
cyclin-dependent kinase inhibitor 1A (p21, Cip1) (CDKN1A), transcript variant 1	NM_000389	1.20	0.139 883	2.58	0.001 035	2.27	0.001 779	2.06	0.004 558
cyclin-dependent kinase inhibitor 1C (p57, Kip2) (CDKN1C)	NM_000076	1.31	0.044 667	2.30	0.000 426	2.74	0.000 725	2.41	0.000 595
polo-like kinase 3 (*Drosophila*) (PLK3)	NM_004073	1.42	0.0307	3.29	7.10×10^{-5}	3.64	0.000 259	3.52	0.004 782
polo-like kinase 2 (*Drosophila*) (PLK2)	NM_006622	1.51	0.036 132	2.92	0.006 303	3.08	0.003 052	2.80	0.004 228
protein phosphatase 2 (formerly 2A), catalytic subunit, β isoform (PPP2CB), transcript variant 2	NM_001009552	1.23	0.241 224	2.42	0.000 508	2.04	0.001 555	2.15	0.004 221
putative lymphocyte G0/G1 switch gene (G0S2)	NM_015714	0.77	0.245 573	0.24	0.000 736	0.23	0.000 445	0.26	0.003 552
v-jun sarcoma virus 17 oncogene homologue (avian) (JUN)	NM_002228	1.92	0.008 419	4.80	0.000 07	4.79	0.000 93	2.76	0.004 977
jun B proto-oncogene (JUNB)	NM_002229	1.23	0.236 543	2.88	0.000 496	2.71	0.001 525	2.28	0.014 609
v-Ki-ras2 Kirsten rat sarcoma viral oncogene homologue (KRAS), transcript variant a	NM_033360	1.08	0.413 903	2.25	0.000 912	1.94	0.002 58	1.56	0.031 253
v-fos FBJ murine osteosarcoma viral oncogene homologue (FOS)	NM_005252	1.70	0.021 487	3.51	0.000 744	2.68	0.004 253	2.92	0.006 751
v-myc myelocytomatosis viral oncogene homologue (avian) (MYC)	NM_002467	1.26	0.140 158	2.00	0.006 322	2.20	0.012 852	3.32	0.003 831
BTG family, member 3 (BTG3)	NM_006806	1.15	0.119 292	2.05	0.012 971	2.16	0.001 447	1.95	0.000 833
headcase homologue (*Drosophila*) (HECA)	NM_016217	1.19	0.046 632	2.03	0.001 548	1.94	0.003 73	1.74	0.003 227
dual specificity phosphatase 4 (DUSP4), transcript variant 1	NM_001394	1.15	0.028 773	1.42	0.000 564	1.32	0.006 108	1.42	0.001 007
proliferating cell nuclear antigen (PCNA), transcript variant 1	NM_002592	0.77	0.112 291	0.56	0.019 576	0.53	0.007 429	0.58	0.015 66
anaphase promoting complex subunit 5 (ANAPC5)	NM_016237	1.02	0.792 272	0.73	0.028 854	0.74	0.035 319	0.77	0.079 311

[a] FC, fold change; GA, glycoalkaloid.

induced was cyclin-dependent kinase inhibitor 1C (CDKN1C or p57 or Kip2), which, similar to CDKN1A, inhibits DNA replication by binding to the proliferating cell nuclear antigen (PCNA), resulting in antiproliferative effects (*37*, *38*). Expression of either Plk3 or CNKN1A can result in either G_2/M or G_0/G_1 arrest; therefore, this may explain the different effects on the cell cycle observed using selected α-chaconine concentrations.

We also observed the differential expression of genes encoding potential regulators/players of proapoptotic/apoptotic or cell-death cascades. Cell death may occur because of either necrotic or apoptotic processes depending upon the cell type and stimulus. Apoptosis is executed mainly by a family of proteases called caspases, which can be activated by two main pathways, i.e., the extrinsic (via cell-surface death receptors) and intrinsic (via perturbation of the mitochondrial membrane) pathways (*39*, *40*). Necrosis is characterized by swelling of the cell and its organelles, resulting in cell-membrane disruption and cell lysis. Downstream mediators of the extrinsic tumor necrosis factor (TNF) pathway were affected by glycoalkaloid treatments in the present study (**Table 4**; TNFRSF1A, TNFRSF11B, TNFRSF12A, and TNFRSF21). TNF was observed to induce, via binding to TNF receptors, either apoptosis or necrosis depending upon cellular context (*41*, *42*). However, we also observed the induction of genes that are involved in the intrinsic mitochondria-mediated apoptotic pathways (**Table 4**; BBC3, BMF, SH3GLB1, and PHLDA1). In addition, Yang et al. observed that, in HT29 cells, α-chaconine induced apoptosis. This effect may be mediated through the suppression of Erk1/2 phosphorylation and subsequent activation of caspase 3. The results obtained with the annexin V assay indicated that α-chaconine exposure resulted in late apoptosis and necrosis rather than early apoptosis in differentiated Caco-2 cells. Thus, both apoptosis and necrosis may have occurred simultaneously.

Many of the genes showing alterations in expression were encoding transcription factors, including NF-κB and activating protein 1 (AP-1) dimers (c-Fos, FosB, c-Jun, JunB, and ATF3). NF-κB activity is stimulated by a wide range of stimuli, such as pathogens, stress signals, and pro-inflam-

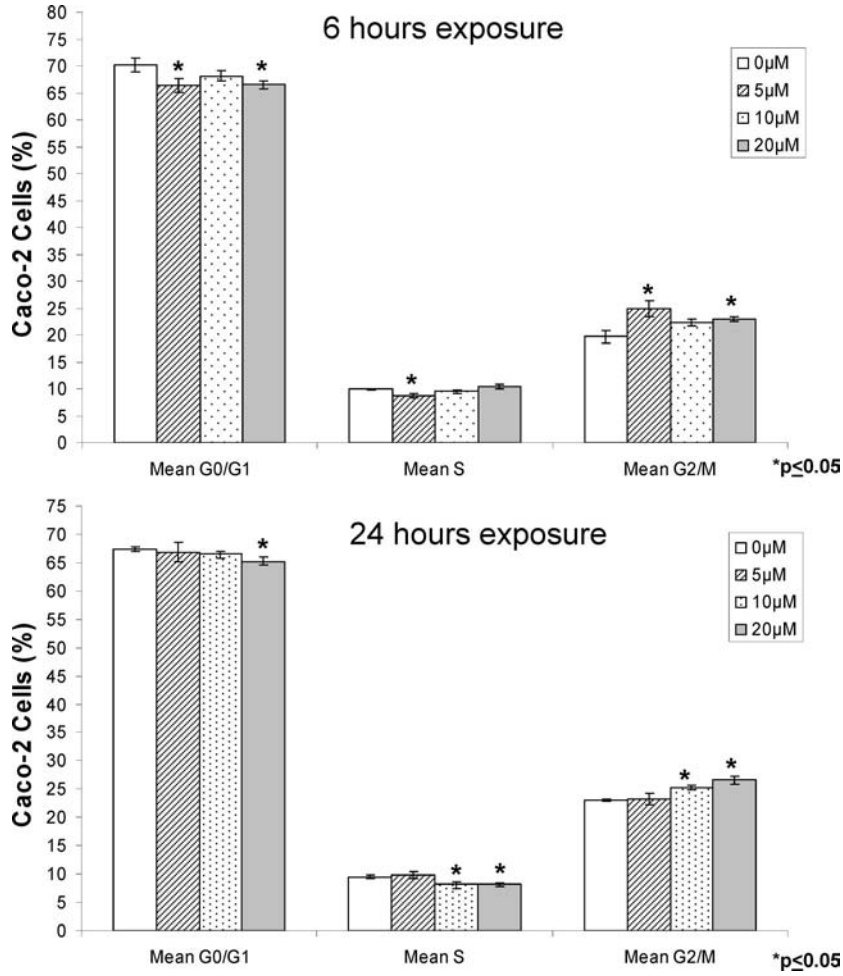

Figure 4. Effect of various concentrations of α-chaconine on the cell-cycle phase in Caco-2 cells. Cells were grown for 19 days and then exposed to 5–20 μM α-chaconine for either 6 or 24 h. Cell-cycle phases were identified by propidium iodide flow cytometry. Values are expressed as mean ± standard deviation (SD). (∗) *p* values shown are in comparison to the values of the control group.

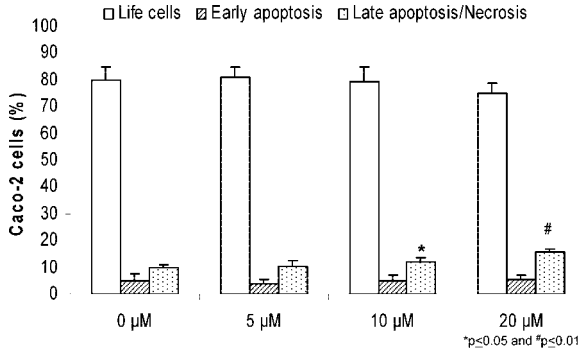

Figure 5. Effect of various concentrations of α-chaconine on apoptosis/necrosis in Caco-2 cells. Cells were grown for 19 days and then exposed to 5–20 μM α-chaconine for 6 h. Values are expressed as mean ± SD. (∗ and #) *p* values shown are in comparison to the values of the control group.)

matory cytokines (*43*). AP-1 activity is induced by growth factors, cytokines, neurotransmitters, bacterial and viral infections, and a variety of physical and chemical stresses (*44*). NF-κB and AP-1 are key transcription factors that regulate the expression of many genes important for diverse processes, for example, cell growth, development, inflammation, stress responses, immune, cell-cycle progression, and apoptosis (*43–45*). Because we observed the differential expression of several genes/processes involved in growth signaling, cell-cycle regulation, apoptosis, and chemokine and cytokine signaling, which are targets of NF-κB and AP-1, it is conceivable that potato glycoalkaloids affect these processes via these transcription factors.

In conclusion, this study describes changes in gene-expression profiles in response to potato glycoalkaloids. Gene-profiling experiments revealed that the glycoalkaloids, α-chaconine and α-solanine, and their mixtures act by the same mechanisms, with the main difference being the degree of potency. Most importantly, we observed the induction of cholesterol biosynthesis genes by non-cytotoxic glycoalkaloid treatments and the repression of their induction by more severe glycoalkaloid concentrations that result in cytotoxicity. Induction of cholesterol biosynthesis genes may be an early response to glycoalkaloid toxicity, induced perhaps to rescue cells from the progression to death. Furthermore, we conclude that microarrays used in conjunction with classical toxicological tests can be useful in discriminating glycoalkaloid treatments on the basis of potency or degree of effect, thus demonstrating the potential of microarray technology as a tool for detecting subtle differences in toxicities of mixtures and/or possibly also whole foods. Mixture studies, such as those performed in the present work, can be helpful to predict the toxicological consequences of changing relative levels of compounds in food crops, for example, changing α-chaconine/α-solanine ratios in potato by genetic modification.

ACKNOWLEDGMENT

We thank Dr. Marjoke Heneweer and Dr. Evert van Schothorst (RIKILT, Wageningen, The Netherlands) for critically reading the manuscript.

LITERATURE CITED

(1) Patel, B.; Schutte, R.; Sporns, P.; Doyle, J.; Jewel, L.; Fedorak, R. N. Potato glycoalkaloids adversely affect intestinal permeability and aggravate inflammatory bowel disease. *Inflammatory Bowel Dis.* **2002**, *8* (5), 340–346.

(2) Friedman, M.; Henika, P. R.; Mackey, B. E. Effect of feeding solanidine, solasodine and tomatidine to non-pregnant and pregnant mice. *Food Chem. Toxicol.* **2003**, *41* (1), 61–71.

(3) Rayburn, J. R.; Bantle, J. A.; Qualls, J., C. W.; Friedman, M. Protective effects of glucose-6-phosphate and NADP against α-chaconine-induced developmental toxicity in *Xenopus* embryos. *Food Chem. Toxicol.* **1995**, *33* (12), 1021–1025.

(4) Roddick, J. G.; Rijnenberg, A. L. Effect of steroidal glycoalkaloids of the potato on the permeability of liposome membranes. *Physiol. Plant.* **1986**, *68* (3), 436–440.

(5) Roddick, J. G.; Rijnenberg, A. L. Synergistic interaction between the potato glycoalkaloids α-solanine and α-chaconine in relation to lysis of phospholipid/sterol liposomes. *Phytochemistry* **1987**, *26* (5), 1325–1328.

(6) Rayburn, J. R.; Bantle, J. A.; Friedman, M. Role of carbohydrate side chain of potato glycoalkaloids in developmental toxicity. *J. Agric. Food Chem.* **1994**, *42* (7), 1511–1515.

(7) Friedman, M.; Rayburn, J. R.; Bantle, J. A. Developmental toxicology of potato alkaloids in the frog embryo teratogenesis assay—*Xenopus* (FETAX). *Food Chem. Toxicol.* **1991**, *29* (8), 537–547.

(8) Morris, S. C.; Lee, T. H. The toxicity and teratogenicity of *Solanaceae* glycoalkaloids, particularly those of the potato (*Solanum tuberosum*): A review. *Food Technol. Aust.* **1984**, *36* (3), 118–124.

(9) Roddick, J. G.; Weissenberg, M.; Leonard, A. L. Membrane disruption and enzyme inhibition by naturally occurring and modified chacotriose-containing *Solanum* steroidal glycoalkaloids. *Phytochemistry* **2001**, *56* (6), 603–610.

(10) Friedman, M.; Henika, P. R.; Mackey, B. E. Feeding of potato, tomato and eggplant alkaloids affects food consumption and body and liver weights in mice. *J. Nutr.* **1996**, *126* (4), 989–999.

(11) Caldwell, K. A.; Grosjean, O. K.; Henika, P. R.; Friedman, M. Hepatic ornithine decarboxylase induction by potato glycoalkaloids in rats. *Food Chem. Toxicol.* **1991**, *29* (8), 531–535.

(12) Gaffield, W.; Keeler, R. F. Craniofacial malformations induced in hamsters by steroidal alkaloids. *J. Nat. Toxins* **1996**, *5* (1), 25–38.

(13) Rayburn, J. R.; Friedman, M.; Bantle, J. A. Synergistic interaction of glycoalkaloids α-chaconine and α-solanine on developmental toxicity in *Xenopus* embryos. *Food Chem. Toxicol.* **1995**, *33* (12), 1013–1019.

(14) Mensinga, T. T.; Sips, A. J. A. M.; Rompelberg, C. J. M.; van Twillert, K.; Meulenbelt, J.; van den Top, H. J.; van Egmond, H. P. Potato glycoalkaloids and adverse effects in humans: An ascending dose study. *Regul. Toxicol. Pharmacol.* **2005**, *41* (1), 66–72.

(15) Dao, L.; Friedman, M. Chlorophyll, chlorogenic acid, glycoalkaloid, and protease inhibitor content of fresh and green potatoes. *J. Agric. Food Chem.* **1994**, *42* (3), 633–639.

(16) Smith, D. B.; Roddick, J. G.; Jones, J. L. Synergism between the potato glycoalkaloids α-chaconine and α-solanine in inhibition of snail feeding. *Phytochemistry* **2001**, *57* (2), 229–234.

(17) Friedman, M.; Lee, K.-R.; Kim, H.-J.; Lee, I.-S.; Kozukue, N. Anticarcinogenic effects of glycoalkaloids from potatoes against human cervical, liver, lymphoma, and stomach cancer cells. *J. Agric. Food Chem.* **2005**, *53* (15), 6162–6169.

(18) Roddick, J. G.; Rijnenberg, A. L.; Osman, S. F. Synergistic interaction between potato glycoalkaloids α-solanine and α-chaconine in relation to destabilization of cell membranes: Ecological implications. *J. Chem. Ecol.* **1988**, *14* (3), 889–902.

(19) McCue, K. F.; Allen, P. V.; Shepherd, L. V. T.; Blake, A.; Whitworth, J.; Maccree, M. M.; Rockhold, D. R.; Stewart, D.; Davies, H. V.; Belknap, W. R. The primary in vivo steroidal alkaloid glucosyltransferase from potato. *Phytochemistry* **2006**, *67* (15), 1590–1597.

(20) McCue, K. F.; Shepherd, L. V. T.; Allen, P. V.; Maccree, M. M.; Rockhold, D. R.; Corsini, D. L.; Davies, H. V.; Belknap, W. R. Metabolic compensation of steroidal glycoalkaloid biosynthesis in transgenic potato tubers: Using reverse genetics to confirm the in vivo enzyme function of a steroidal alkaloid galactosyltransferase. *Plant Sci.* **2005**, *168* (1), 267–273.

(21) Dybing, E.; Doe, J.; Groten, J.; Kleiner, J.; O'Brien, J.; Renwick, A. G.; Schlatter, J.; Steinberg, P.; Tritscher, A.; Walker, R.; Younes, M. Hazard characterisation of chemicals in food and diet: Dose response, mechanisms and extrapolation issues. *Food Chem. Toxicol.* **2002**, *40* (2–3), 237–282.

(22) Marchant, G. E. Toxicogenomics and toxic torts. *Trends Biotechnol.* **2002**, *20* (8), 329–332.

(23) Mandimika, T.; Baykus, H.; Poortman, J.; Garza, C.; Kuiper, H.; Peijnenburg, A. Induction of the cholesterol biosynthesis pathway in differentiated Caco-2 cells by the potato glycoalkaloid α-chaconine. *Food Chem. Toxicol.* **2007**, *45* (10), 1918–1927.

(24) Ekins, S.; Andreyev, S.; Ryabov, A.; Kirillov, E.; Rakhmatulin, E. A.; Sorokina, S.; Bugrim, A.; Nikolskaya, T. A combined approach to drug metabolism and toxicity assessment. *Drug Metab. Dispos.* **2006**, *34* (3), 495–503.

(25) Lee, H.; Braynen, W.; Keshav, K.; Pavlidis, P. ErmineJ: Tool for functional analysis of gene expression data sets. *BMC Bioinf.* **2005**, *6* (1), 269.

(26) Koopman, G.; Reutelingsperger, C.; Kuijten, G.; Keehnen, R.; Pals, S.; van Oers, M. Annexin V for flow cytometric detection of phosphatidylserine expression on B cells undergoing apoptosis. *Blood* **1994**, *84* (5), 1415–1420.

(27) Keukens, E. A. J.; de Vrije, T.; Fabrie, C. H. J. P.; Demel, R. A.; Jongen, W. M. F.; de Kruijff, B. Dual specificity of sterol-mediated glycoalkaloid induced membrane disruption. *Biochim. Biophys. Acta* **1992**, *1110* (2), 127–136.

(28) Keukens, E. A. J.; de Vrije, T.; Jansen, L. A. M.; de Boer, H.; Janssen, M.; de Kroon, A. I. P. M.; Jongen, W. M. F.; de Kruijff, B. Glycoalkaloids selectively permeabilize cholesterol containing biomembranes. *Biochim. Biophys. Acta* **1996**, *1279* (2), 243–250.

(29) Keukens, E. A. J.; de Vrije, T.; van den Boom, C.; de Waard, P.; Plasman, H. H.; Thiel, F.; Chupin, V.; Jongen, W. M. F.; de Kruijff, B. Molecular basis of glycoalkaloid induced membrane disruption. *Biochim. Biophys. Acta* **1995**, *1240* (2), 216–228.

(30) Yang, S.-A.; Paek, S.-H.; Kozukue, N.; Lee, K.-R.; Kim, J.-A. α-Chaconine, a potato glycoalkaloid, induces apoptosis of HT-29 human colon cancer cells through caspase-3 activation and inhibition of ERK 1/2 phosphorylation. *Food Chem. Toxicol.* **2006**, *44* (6), 839–846.

(31) Wang, Q.; Xie, S.; Chen, J.; Fukasawa, K.; Naik, U.; Traganos, F.; Darzynkiewicz, Z.; Jhanwar-Uniyal, M.; Dai, W. Cell cycle arrest and apoptosis induced by human polo-like kinase 3 is mediated through perturbation of microtubule integrity. *Mol. Cell. Biol.* **2002**, *22* (10), 3450–3459.

(32) Xie, S.; Wu, H.; Wang, Q.; Cogswell, J. P.; Husain, I.; Conn, C.; Stambrook, P.; Jhanwar-Uniyal, M.; Dai, W. Plk3 functionally links DNA damage to cell cycle arrest and apoptosis at least in part via the p53 pathway. *J. Biol. Chem.* **2001**, *276* (46), 43305–43312.

(33) Martin-Castellanos, C.; Moreno. Recent advances on cyclins, CDKs and CDK inhibitors. *Trends Cell Biol.* **1997**, *7* (3), 95–98.

(34) Guadagno, T. M.; Newport, J. W. Cdk2 kinase is required for entry into mitosis as a positive regulator of Cdc2–cyclin B kinase activity. *Cell* **1996**, *84* (1), 73–82.

(35) Ling, Y.-H.; Liebes, L.; Jiang, J.-D.; Holland, J. F.; Elliott, P. J.; Adams, J.; Muggia, F. M.; Perez-Soler, R. Mechanisms of proteasome inhibitor PS-341-induced G2-M-phase arrest and apoptosis in human non-small cell lung cancer cell lines. *Clin. Cancer Res.* **2003**, *9* (3), 1145–1154.

(36) McShea, A.; Samuel, T.; Eppel, J.-T.; Galloway, D. A.; Funk, J. O. Identification of CIP-1-associated regulator of cyclin B (CARB), a novel p21-binding protein acting in the G2 phase of the cell cycle. *J. Biol. Chem.* **2000**, *275* (30), 23181–23186.

(37) Waga, S.; Hannon, G. J.; Beach, D.; Stillman, B. The p21 inhibitor of cyclin-dependent kinases controls DNA replication by interaction with PCNA. *Nature* **1994**, *369* (6481), 574–578.

(38) Watanabe, H.; Pan, Z.-Q.; Schreiber-Agus, N.; DePinho, R. A.; Hurwitz, J.; Xiong, Y. Suppression of cell transformation by the cyclin-dependent kinase inhibitor p57KIP2 requires binding to proliferating cell nuclear antigen. *Proc. Natl. Acad. Sci. U.S.A.* **1998**, *95* (4), 1392–1397.

(39) Thorburn, A. Death receptor-induced cell killing. *Cell. Signalling* **2004**, *16* (2), 139–144.

(40) Wang, X. The expanding role of mitochondria in apoptosis. *Genes Dev.* **2001**, *15* (22), 2922–2933.

(41) Laster, S.; Wood, J.; Gooding, L. Tumor necrosis factor can induce both apoptic and necrotic forms of cell lysis. *J. Immunol.* **1988**, *141* (8), 2629–2634.

(42) Fiers, W.; Beyaert, R.; Declercq, W.; Vandenabeele, P. More than one way to die: Apoptosis, necrosis and reactive oxygen damage. *Oncogene* **1999**, *18* (54), 7719–7730.

(43) Li, Q.; Verma, I. M. NF-κB regulation in the immune system. *Nat. Rev. Immunol.* **2002**, *2* (10), 725–734.

(44) Shaulian, E.; Karin, M. AP-1 as a regulator of cell life and death. *Nat. Cell Biol.* **2002**, *4* (5), E131–E136.

(45) Fujioka, S.; Niu, J.; Schmidt, C.; Sclabas, G. M.; Peng, B.; Uwagawa, T.; Li, Z.; Evans, D. B.; Abbruzzese, J. L.; Chiao, P. J. NF-κB and AP-1 connection: Mechanism of NF-κB-dependent regulation of AP-1 activity. *Mol. Cell. Biol.* **2004**, *24* (17), 7806–7819.

Received for review August 13, 2007. Accepted September 27, 2007. The authors thank the European Union (NOFORISK FOOD-CT-2003-506387), Cornell University, and the Dutch Ministry of Agriculture, Nature, and Food Quality for funding this research.

JF0724320